Study on thermal storage effectiveness of a novel PCM concrete applied in buildings located at four cities

Xinghai Liu, Yingying Yang, Zhonghua Sheng, Weidong Wu, Yuan Wang, Jean Dumoulin

Numerical Study of thermal performances for a novel PCM concrete applied in building envelope

Xinghai LIU[1], Yingying YANG[1,2*], Zhonghua SHENG[1], Weidong WU[1,2*], Yuan WANG[3], Jean DUMOULIN[4]

[1]School of Energy and Power Engineering, University of Shanghai for Science and Technology, Shanghai 200093, China

[2]Shanghai Key Laboratory of Multiphase Flow and Heat Transfer in Power Engineering, Shanghai 200093, China

[3]Department of Building Science, School of Architecture, Tsinghua University, Beijing Key Laboratory of Indoor Air Quality Evaluation and Control, Beijing 100084, China

[4]University Gustave Eiffel, Inria, COSYS-SII, I4S Team, F-44344 Bouguenais, France

Abstract: The implementation of phase change thermal storage technology represents a high potential strategy for mitigating energy consumption and reducing thermal and cooling loads in buildings. However, the effectiveness of such technology is greatly influenced by the outdoor thermal environmental conditions specific to each location, necessitating further investigation over longer duration. In this research, a novel phase change material (PCM), named LA-SA/Al_2O_3/C, was integrated into building envelopes. Numerical simulations were conducted to assess the impact of PCM concrete on the thermal performance of multi-storey building walls for a period of up to one year, considering four distinct climate zones. The findings reveal that the novel PCM concrete demonstrates maximum effectiveness in Paris, effectively reducing indoor temperatures and temperature fluctuations during the summer season. Conversely, in the remaining regions, where high overall outdoor temperatures prevail during summer, the PCM within the walls remains in a molten state, unable to solidify and effectively absorb heat. Consequently, the thermal performance of the phase change walls in these regions is not favorable during summer, but rather during the transitional seasons of spring and autumn. In summary, the new PCM concrete exhibits the capacity

to reduce heat transfer through walls; however, the thermal performance is primarily dictated by the solar-air outdoor temperature. Therefore, in order to maximize the latent heat storage potential of phase change materials, the selection of appropriate PCM with optimal phase change temperature zones becomes crucial, particularly when implementing this technology in diverse climatic zones.

Keyword: Thermal storage; PCM; Concrete; Building energy conservation

1. Introduction

Global building energy consumption accounts for approximately one-third of the total social energy consumption. Among building energy consumption, more than half is attributed to indoor environment control, namely heating and cooling. This proportion is expected to increase as people's expectations for indoor environmental comfort continue to rise. In term of buildings, the heat and cold loss from the building envelope is the main component of the building heat and cold load. Thus, enhancing the thermal performance of the building envelope is crucial for reducing building load and energy consumption.

Phase Change Material (PCM) can absorb or release energy to keep the temperature constant during the phase change process. Integrating PCM into the building envelope can effectively enhance the thermal storage capacity of the building and improve the building energy efficiency. Both experimental and simulation studies have confirmed the promising applications of PCM in achieving energy efficiency and improving indoor environmental comfort in buildings [1-3]. PCM has been reported to be integrated into various building envelopes such as walls [4], bricks [5], windows [6], floor [7], ceilings [8], concrete [9], mortar [10], and gypsum boards [11] to improve the thermal mass of the building envelope. This enables storing more energy within the same mass of the building. The latent heat stored or released by PCM can significantly

reduce building energy consumption, promote efficient energy utilization, and enhance thermal comfort through effective temperature regulation.

Over the past decade, many experts and scholars have conducted experimental and simulation studies on the effects of PCM in building envelopes. For example, Sun et al. [12] developed a new PCM material using expanded perlite as a shell, improving the thermal storage performance and structural stability of PCM for temperature control purposes. Mohammad et al. [13] investigated the effect of enhanced PCM envelopes on the thermal performance of building envelopes. The results showed that the enhanced PCM envelopes can provide optimal cooling demand conversion and energy flexibility efficiency for the building envelope. Lisa et al. [14] compiled different kinds of PCM from around the world, as well as re-examining the parameters used for PCM selection and emphasizing the importance of proper selection and placement of PCM within the building structure to reduce energy consumption.

The thermal performance and energy efficiency of PCM vary under different climatic conditions and installation locations. Zu et al. [15] investigated the patterns and effects of different PCM types and configurations on the thermal performance of lightweight building walls during summer and winter. The results pointed out that for the same PCM thickness, double-layered PCM had the best thermal regulation capacity when placed in the middle of the wall and was more prominent in summer. Qudama et al. [16] quantified the effect of PCM on the thermal regulation and energy saving in building envelopes under extreme hot conditions. They found that PCM effectively reduced indoor temperature and heat load, particularly when placed on the roof compared to the walls. Loucas et al. [17] investigated the optimal placement of PCM wall coatings. It was revealed that in warm climates, the coating was most effective on the east and west sides; while in cold climates, the north side was most effective, with

the coating placed on the outer side of the wall. Liu et al. [18] produced a small lightweight building and tested the effect of PCM location and parameters on the thermal performance of the building wall in different directions. The test concluded that the optimal location for PCM was in the middle of the east and south facing walls, while the east and west facing walls exhibiting the most significant improvement in thermal performance when using appropriate PCM parameters. Moreover, numerical simulation methods have been employed to study PCM due to their ability to enhance testing speed and expand the testing area compared to traditional experimental methods. For instance, Haruka et al. [19] developed a coupled simulation model combining heat balance analysis and computational fluid dynamics simulation for a naturally ventilated building with PCM installation. The simulations closely matched actual measurements of air temperature, as well as the temperature and heat balance of PCM in the building. Ching et al. [20] simulated the effect of PCM foam cement walls on the thermal performance and economy of single-story buildings in five different climate zones in China. The results showed that PCM foam cement exhibited thermal and energy-saving performance on all five climate zones, with the highest energy savings in Kunming but the longest application payback period. Li et al. [21] simulated the effect of embedding PCM into conventional building walls, revealing that wall heat transfer decreased with increasing PCM thickness, emphasizing the significance of thermal conductivity compared to other physical parameters. Xie et al. [22] simulated the performance of five types of PCM wall panels on the exterior wall of a room in Beijing, highlighting the improved thermal performance of PCM wall panels during certain months, with different optimal phase change ranges for each month.

In summary, although many scholars have already made progress through experimental and simulation studies on phase change energy storage materials, but

limited by the cost issue, most experimental studies are only developed to laboratory scale building models. So it is difficult to build real PCM buildings or demonstration projects, as well as evaluating the actual application effect. Meanwhile, existing simulation cases often focus on specific walls or partial walls, such as bricks, failing to reflect the full energy-saving potential of PCM when applied to real buildings. Moreover, many simulation studies are of short duration, typically lasting only a few weeks or months under typical hot summer conditions. Few studies consider year-round climatic conditions or the effects of year-round applications of the same PCM envelope in different cities.

To address the above situation, this study adopts a phase change composite material named LASA/Al_2O_3/C, embedded in cement mortar to develop a storage-reinforced PCM concrete. The thermal properties of this concrete are experimentally tested, and a 3D house model comprising normal concrete and PCM concrete is established for simulation studies. Then, taking four different climate zones as example to simulate the indoor air temperature fluctuation and heat flow of the PCM concrete house and the normal concrete house up to one year, so as to explore the practical application potential and analyze the effectiveness of this novel PCM concrete, and provide valuable insights for the application of this PCM concrete.

2. Model of the PCM house

2.1 Physical model

The structural model of the house is depicted in Fig. 1[a]. The dimensions of both the normal concrete and PCM concrete houses are 5 m × 5 m × 3.5 m(height). Each room has a flat roof with a south-facing glass window measuring 2.5 m × 1.5 m and a solid wood exterior door on the north-facing wall measuring 1.5 m × 2.5 m.

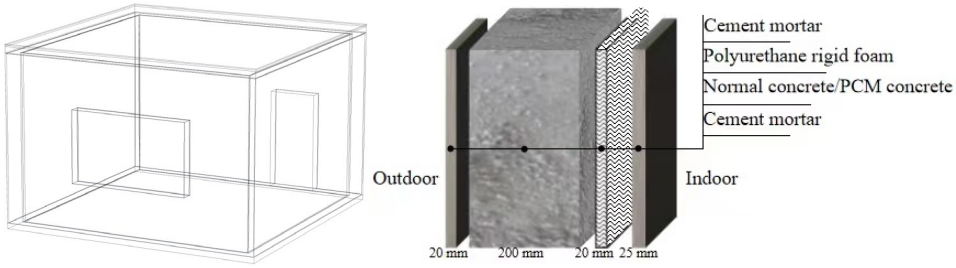

[a] 3D model [b] Wall structure

Fig.1. The [a][b] of the house with normal concrete/PCM concrete

The multi-layer wall structures of the houses are illustrated in Fig 1[b]. For simplicity, the floors of both houses consist of single concrete layers since they do not exchange heat with the outdoor thermal environment in this simulation. The physical parameters of the material in each layer of the wall and roof structure of the house model are shown in Table 1.

Table 1 Thermal performance parameters for each layer of material

Materials	ρ /kg·m^{-3}	C_P /J·(kg·K)$^{-1}$	K /W·(m·K)$^{-1}$
Cement mortar	1800	1050	0.93
Normal concrete	2170	1030	1.39
Polyurethane rigid foam	30	1380	0.027
EPS extruded board	35	1380	0.028
Concrete pressed roof slab	2300	920	1.51
Glass window	2500	750	1
Wooden door	532	2700	0.11
Solid PCM concrete	1560	1218	1.12
Liquid PCM concrete	1560	1237	1.12

To facilitate calculations and mathematical modelling, the following assumptions were made for the phase change house simulation:

(1)The initial temperature and material of the house are homogeneous.

(2)The thermal physical parameters of PCM do not change with temperature in a single phase.

(3)Neglect the density change during the phase change of the phase change material.

(4)The air temperature is uniform in all parts of the room, i.e. the indoor air is considered as a whole.

(5)The house is a passive construction that does not consider the interior active temperature regulation.

2.2 Mathematical models

The thermal conductivity control equation for the mathematical model utilized in this paper is as follows:

$$\rho C_p \frac{\partial T}{\partial \tau} = \nabla \cdot (k \nabla T) \quad (1)$$

Where, ρ—material density, kg·m^{-3};

C_p—material heat capacity, J·(kg·K)$^{-1}$;

k—thermal conductivity, W·(m·K)$^{-1}$;

T—Temperature, K.

Energy equation:

$$\rho C_p \frac{\partial T}{\partial \tau} + \rho C_p u \cdot \nabla T = \nabla \cdot (k \nabla T) \quad (2)$$

Liquid fraction f_l and solid fraction f_2 of PCM during phase change：

$$f_1 = \begin{cases} 0 & T \le T_s \\ \dfrac{T - T_s}{T_l - T_s} & T_s < T < T_l \\ 1 & T \ge T_l \end{cases} \quad (3)$$

$$f_1 + f_2 = 1 \quad (4)$$

Where, T_S、T_l—Starting and ending temperatures of the melting phase change process, K

Based on the liquid fraction of the PCM, the heat capacity of the PCM is obtained:

$$c_{\mathrm{p,pcm}} = \frac{1}{\rho}\left(f_1\rho_l c_{\mathrm{p,l}} + (1-f_1)\rho_s c_{\mathrm{p,s}}\right) + L\frac{\partial \alpha_m}{\partial T} \quad (5)$$

$$\alpha_m = \frac{1}{2}\cdot\frac{f_2\rho_s - f_1\rho_l}{f_1\rho_l + f_2\rho_s} \quad (6)$$

Where, ρ_l、ρ_s—Liquid and solid phase densities of PCM, kg/m^3；

$c_{p,l}$、$c_{p,s}$—Constant pressure heat capacity of liquid and solid phases, kJ/(kg·K)；

L—Latent heat of phase change process, J/g；

α_m—Volume fraction of PCM.

Exterior side surface boundary conditions:

$$q_{out} = h_{out}(T_{sol,air} - T_{out,wall}) \quad (7)$$

Interior side surface boundary conditions:

$$q_{in} = h_{in}(T_{room} - T_{in,wall}) \quad (8)$$

Where, h_{out}—Heat transfer coefficient of the external surface of the envelope, taken as 22.3[W/(m^2·K)] [23]；

h_{in}—Heat transfer coefficient of the internal surface of the envelope, taken as 12.3[W/(m^2·K)]；

$T_{sol,air}$—Solar-air temperature,calculated according to the following equation [21], neglecting solar reflected radiation and atmospheric long-wave radiation heat exchange:

$$T_{sol-air} = \frac{G \times a_s}{h_{out}} + T_a \quad (9)$$

Where, T_a—Outdoor ambient temperature,℃；

G—Horizontal surface transient solar radiation;

a_s—The surface absorption rate, which is taken as 0.65 for external walls and 1

for windows.

2.3 Climatic conditions considered

In order to examine the thermal performance of PCM concrete under diverse climatic conditions, several cities representing different climate types have been selected for comparative analysis. This study considers four typical cities: Paris, Guangzhou, Beijing, and Hangzhou. Paris has a temperate maritime climate, which represents coastal cities in Europe, America, and Oceania. In China, the population is mainly located in the cold zone, temperate zone and hot summer and warm winter zone. Guangzhou, Beijing, and Hangzhou are representative cities in these three climatic zones. Guangzhou in southern China has a subtropical maritime monsoon climate, Beijing has a typical north temperate semi-humid continental monsoon climate, and Hangzhou has a subtropical monsoon climate.

2.4 Thermal properties of PCM concrete considered

The PCM concrete used in this simulation study was a new phase change composite material named LASA/Al_2O_3/C, which was prepared according to a previous study [23]. The proposed PCM was prepared by melt blending method at 82% LA, 18%SA and 0.5 wt% Al_2O_3. This enhanced binary PCM was then vacuum adsorbed into the ceramic pellets, covered with a benzine emulsion to prevent PCM leakage, and finally coated with dry cement powder before the benzine emulsion fully set. The resulting composite set PCM is presented in Fig. 2. The phase change temperature of the composite fixed PCM was 22.5°C and the latent heat of phase changing process was 133.4 kJ/kg, representing an increase compared to the ceramic encapsulated fixed PCM at the same phase change temperature range [24,25].

Fig.2. LASA/Al_2O_3/C

PCM concrete was prepared by incorporating the above-mentioned composite shaped PCMs, and its thermal properties are shown in Table 2. Fig. 3 shows the DSC curves of LASA/Al_2O_3/C and comparison with that of LA-SA/Al_2O_3. The thermal conductivity of normal concrete is 1.39 W/(m·K), after adding the PCM, the thermal conductivity of PCM concrete decreases to 1.12 W/(m·K), reflecting a 19.4% reduction in thermal conductivity. This significant difference in thermal conductivity is primarily attributed to the low thermal conductivity of LASA/Al_2O_3/C.

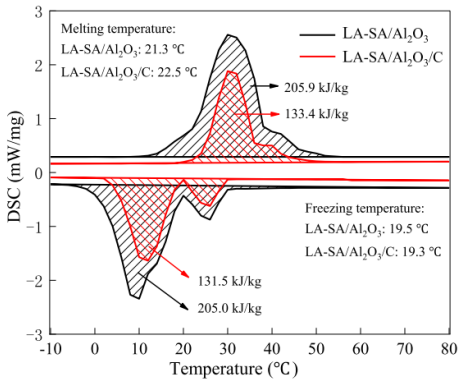

Fig. 3. DSC results of LASA/Al_2O_3 and LASA/Al_2O_3/C.

Table2 Thermal properties of the concrete

Type of the concrete	Thermal conductivity (W/m·K)	Thermal diffusivity (mm^2/s)	Specific heat capacity (kJ/kg·K)
Normal concrete	1.39	11.34	1.03
PCM concrete	1.12	10.86	1.01

2.5 Model validation

Using the proposed mathematical model, a physical simulation was conducted based on a previous experimental study [26]. The simulation results were meticulously

compared with the corresponding experimental data from the previous study. In the experimental setup, a concrete panel was subjected to heating from a heater placed on one side (referred to as the hot side), while the lateral sides of the panel were covered with insulation panels to maintain a one-dimensional heat transfer condition. The opposite side of the panel (referred to as the cold side) was exposed to the surrounding environment. Captec heaters and heat flux meters equipped with built-in T-type thermocouples were employed to measure heat flux and temperature. The experimental setup for evaluating the thermal performance of the concrete panel is depicted in Fig. 4

To simulate the thermal behavior of PCM concrete, a simplified model considering melting and solidification processes without accounting for PCM convection was utilized. The validity of the simplified model was confirmed through comparison with the experimental data from the previous study. During the validation process, an external convective heat transfer coefficient of 20 W/(m^2·K) was assumed for the blocks, while the initial temperature and ambient temperature were both set to 18°C. The experimental results for the cold side of both normal concrete and PCM concrete were compared with the numerical simulation results. The comparison revealed excellent agreement between the predictions of the simplified model and the experimental observations. It was observed that the temperature on the cold side increased over time for both experimental and numerical data. The temperature profile of PCM concrete exhibited a smoother trend with lower peak temperatures compared to that of the normal concrete. The maximum relative deviation between the experimental and numerical results for the cold side temperature was found to be 1.86% for normal concrete and 4.94% for PCM concrete. This minor deviation could be attributed to potential insulation imperfections during the experiments, such as gaps between the insulation panels and the test blocks. Nevertheless, the deviation remained

within the acceptable margin of 5%, thus affirming the validity and accuracy of the proposed model.

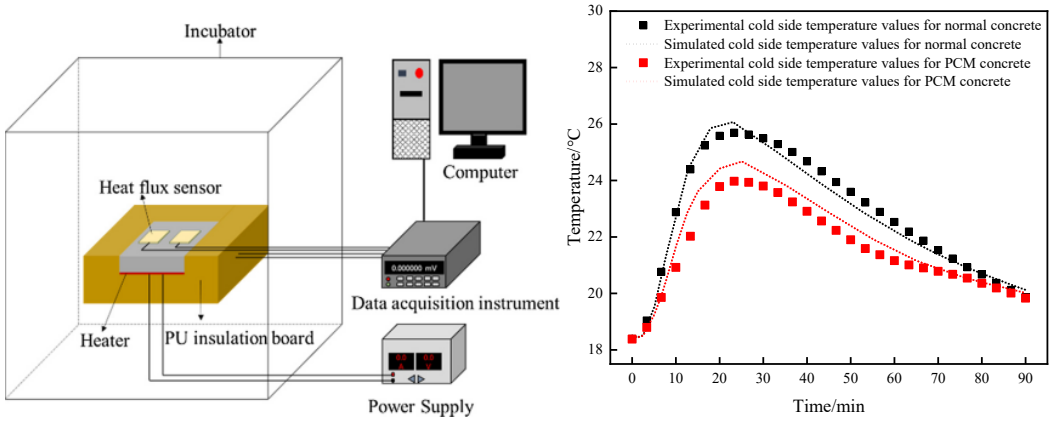

[a] Thermal performance test system [b] warming - cooling curve

Fig. 4. The [a] [b] of the PCM concrete

3. Simulation results

3.1 Paris

3.1.1 Indoor temperature and liquid fraction variation

Paris is located in the center of the Paris Basin in northern France and has a temperate marine climate, mild and humid all year round, with an annual average temperature of 12.7°C. The average temperatures in January and July are around 5°C and 21°C. Fig. 5[a] shows the annual outdoor ambient temperature and the variation in horizontal solar radiation in the region, while Fig. 5[b] shows daily average solar-air temperature.

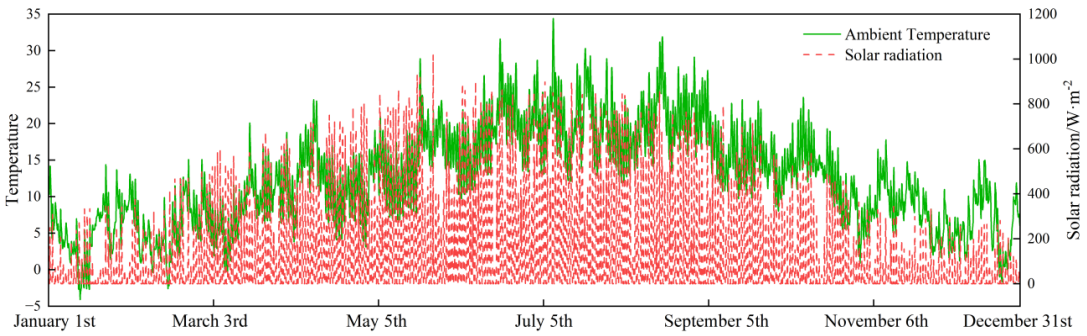

[a] Outdoor temperature and solar horizontal radiation

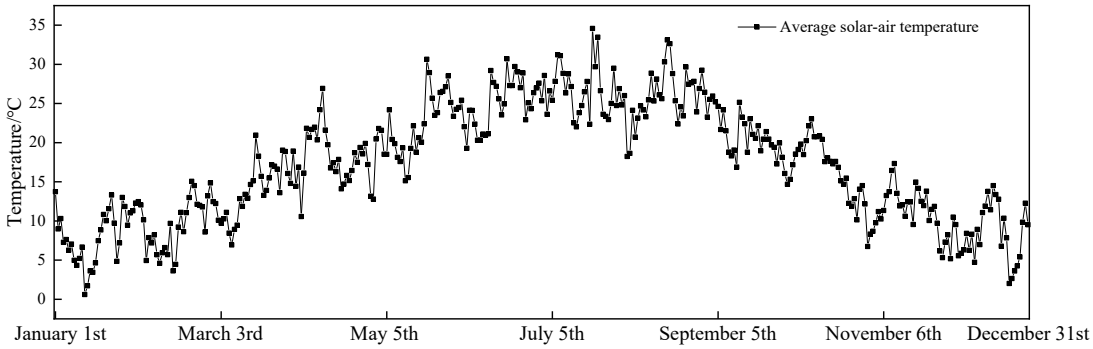

[b] Daily average solar-air temperature

Fig. 5[c] and Fig. 5[d] present the annual variation in indoor temperatures for both the normal concrete house and the PCM concrete house, as well as the liquid fraction of PCM concrete in Paris. By analyzing Fig. 5[c] and Fig. 5[d], it can be concluded that the liquid fraction of the PCM concrete reached higher from June to September each year. Consequently, the PCM was better utilized during this period, leading to lower indoor temperatures and reduced temperature fluctuations in the PCM concrete house throughout the year (Fig. 5[d]). This comparison effectively demonstrates the temperature regulation capability of PCM.

However, during other times of the year, the liquid fraction of the PCM concrete remained 0 for most of the time due to the outdoor temperature not reaching the phase change temperature of the PCM concrete. Nevertheless, the indoor temperature of the PCM concrete house still differed from that of the normal concrete house. This discrepancy can be attributed to the distinct physical properties of the PCM concrete, such as thermal conductivity, resulting in higher indoor temperatures for the PCM concrete house during winter compared to the normal concrete house.

To assess the extent of PCM utilization in the wall, the liquid fraction is divided into three intervals based on percentage: 20% to 40% indicates partial PCM utilization, 40% to 80% indicates effective PCM utilization, and 80% to 100% indicates full PCM utilization. Fig. 5[d] shows the number of hours corresponding to each liquid fraction

interval. The liquid fraction surpassed 20% for 1054 hours, approximately 12% of the year. Furthermore, it exceeded 40% for 631 hours, approximately 7.2% of the year, and reached above 80% for 220 hours, approximately 2.5% of the year, indicating well PCM utilization throughout the year. The time period where the liquid fraction exceeded 20% was primarily concentrated in the summer months, from early June to early September, coinciding with 57 days when the average daily solar-air outdoor temperature reached 25°C. These 57 days account for approximately 65.52% of the time period and are selected as the typical interval for analysis.

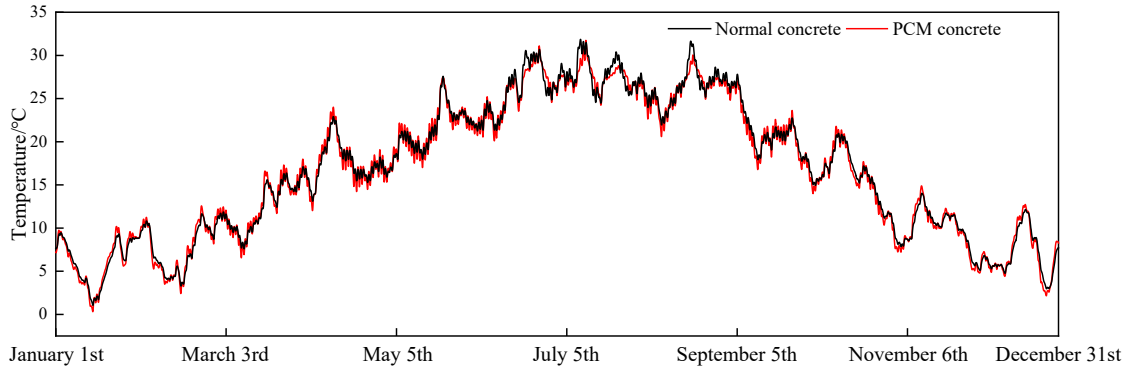

[c] Indoor temperature

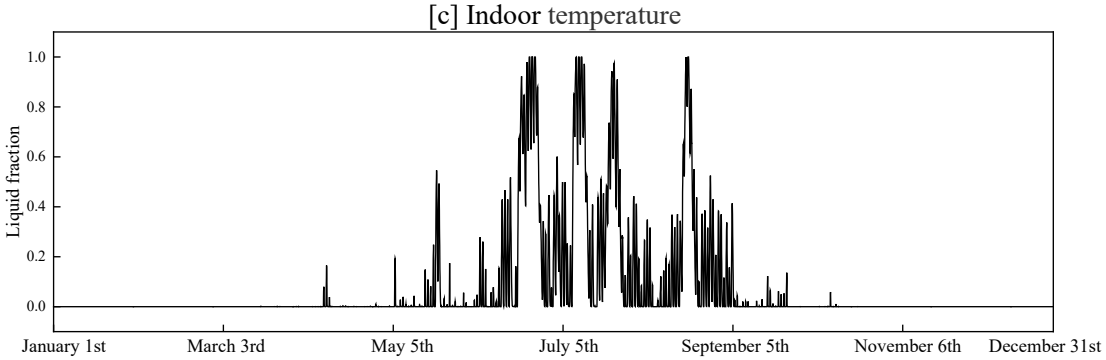

[d] Liquid fraction

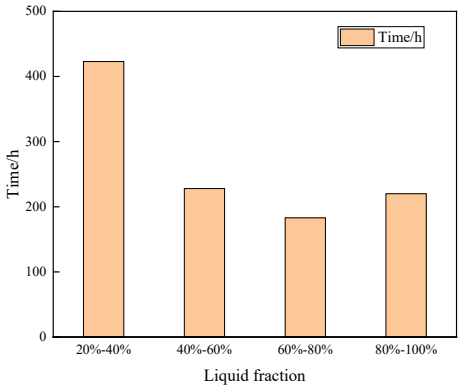

[e] Hours accounted for different liquid fraction percentages

Fig. 5. Full-year variations in [a] [b] [c] [d] [e] in Paris

3.1.2 Typical interval analysis

Fig. 6[a] presents the average solar-air temperature, daily temperature difference between day and night, and the liquid fraction variation in Paris from June 12th to September 7th (days). The solar-air temperature in Paris during this time period exhibited considerable fluctuations. The duration with a temperature difference greater than 20°C amounted to 69 days, accounting for 79.31% of the total time in this interval. Moreover, the duration with a temperature difference exceeding 30°C reached 19 days, representing 21.83% of the total time. Meanwhile, the average solar-air temperature difference during this interval was 24.97°C, with an average solar-air temperature surpassing 25°C for 65.52% of the duration. Analyzing the liquid fraction variation in Fig. 6[a], it is evident that the liquid fraction underwent significant and continuous changes throughout this interval, reflecting the continuous phase change process in the PCM concrete. It is shown that the liquid fraction exceeding 20% for 47.8% of the time, surpassing 40% for 29.13% of the time, and reaching above 80% for 10.42% of the time. Consequently, it can be concluded that the PCM was effectively utilized during this summer interval.

Fig. 6[b] and Fig. 6[c] depict the comparison of the interior wall temperatures and indoor air temperatures between the normal concrete and PCM concrete houses for this interval. In Fig. 6[b], the average interior wall surface temperature was 27.1°C for the normal concrete and 26.9°C for the PCM concrete. The utilization of PCM concrete resulted in a slight reduction in the average interior wall surface temperature. Additionally, the PCM concrete exhibited less fluctuation in interior wall surface temperature compared to the normal concrete. Furthermore, the PCM concrete had more instances with lower temperatures than the normal concrete, with a maximum

temperature difference of 2.49°C. The variance of the interior wall surface temperature of the PCM concrete was 2.92 in this interval, whereas the normal concrete had a variance of 4.07. Thus, the application of the PCM concrete significantly reduced the fluctuation of the interior wall surface temperature.

During this interval, the interior wall surface temperature of the normal concrete exceeded 28°C for up to 597h, while the PCM concrete maintained such high temperatures for 509 hours, resulting in a noticeable reduction in the duration of high interior wall surface temperature. As depicted in Fig. 6[c], the temperature changes in the interior wall were reflected in the indoor air temperature. Thus, the indoor temperature of the PCM concrete house remained lower than that of the normal concrete house for most of the time, reaching 1564h, which is approximately 74.9% of the interval. The graph also reveals the difference in indoor temperature, with the indoor temperature difference between the PCM concrete and the normal concrete exceeding 2°C for 68 hours. The average indoor air temperature for the normal concrete house and PCM concrete house was 27.09 and 26.76, with a variance of 4.01 and 3.20 respectively. These findings demonstrate the significant effect of PCM concrete in reducing indoor temperature and minimizing temperature fluctuations.

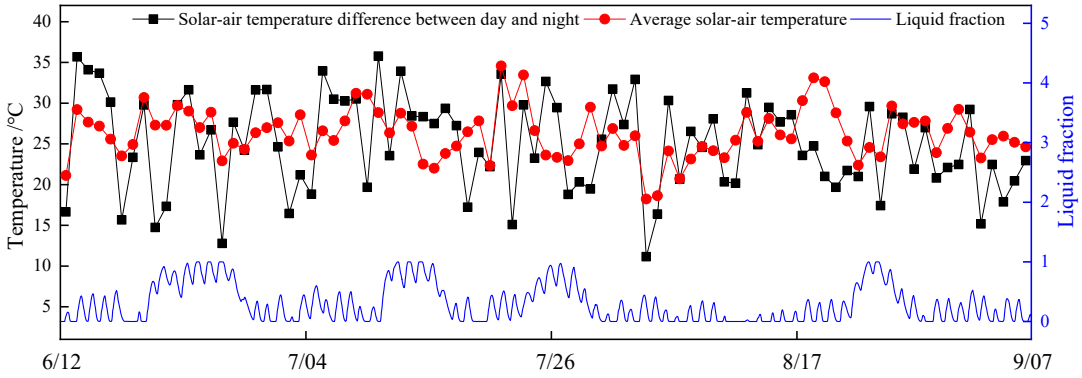

[a] Average solar-air temperature, daily temperature difference between day and night and liquid fraction

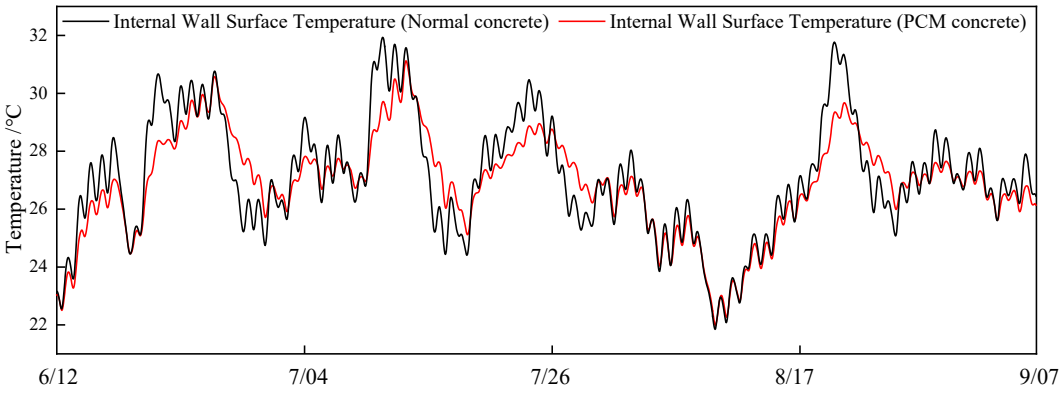

[b] Interior wall surface temperature

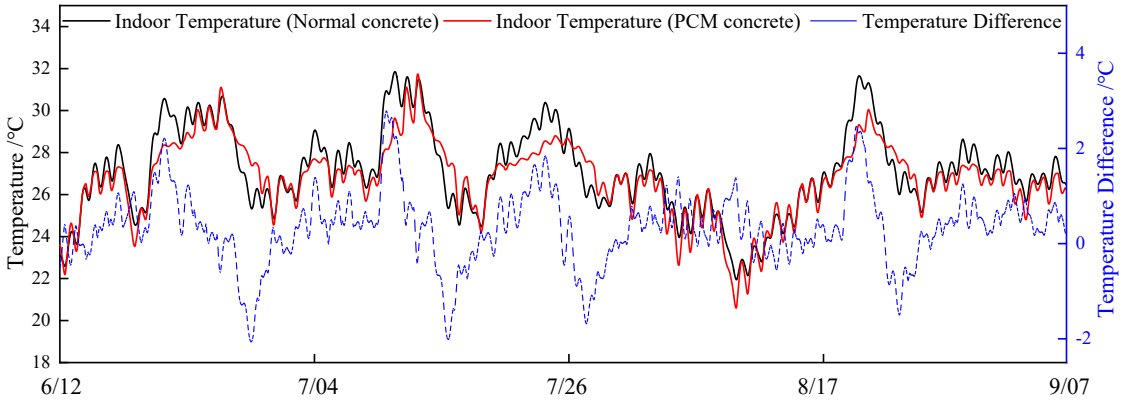

[c] Indoor temperature

Fig. 6. The variation of the [a] [b] [c] between two houses in Paris from June 12th to September 7th

3.2 Guangzhou

3.2.1 Variation in indoor temperature and liquid fraction throughout the year

Guangzhou is located in southern China and has a subtropical maritime monsoon climate, which has hot summers and warm winters with mild temperatures, with an annual average temperature of 23°C. The average temperatures in January and July are approximately 14°C and 29°C respectively. Fig. 7[a] illustrates the annual outdoor temperature and solar horizontal radiation variation in the region, while Fig. 7[b] depicts the daily average solar-air temperature.

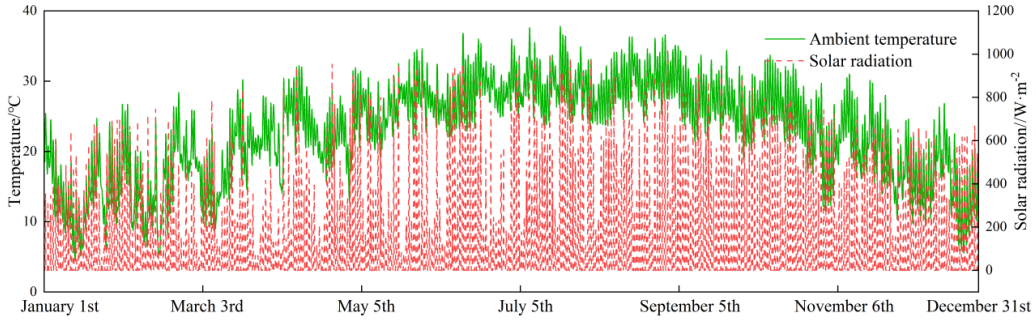

[a] Outdoor temperature and solar horizontal radiation

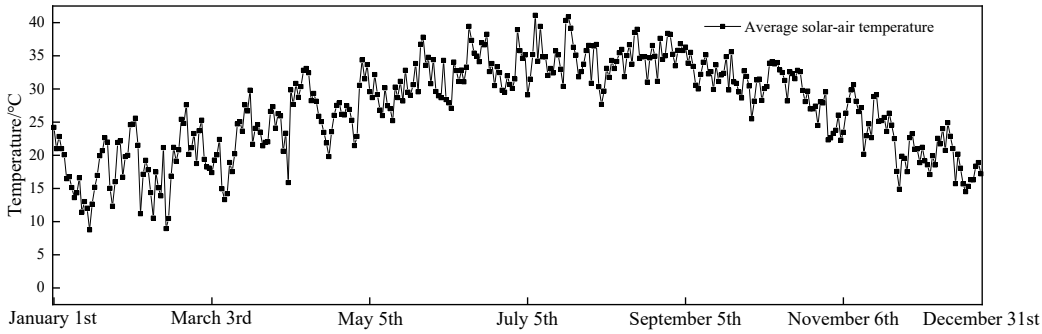

[b] Daily average solar-air temperature

Fig. 7[c] and 7[d] show the yearly variation in indoor temperatures for a normal concrete house and a PCM concrete house, as well as the liquid fraction of PCM concrete in Guangzhou. Based on Fig. 7[c] and 7[d], it can be concluded that the liquid fraction of PCM concrete remained higher from April to November throughout the year. Notably, the liquid fraction exceeded 80% for 4122 hours, accounting for approximately 42% of the year, surpassing the levels observed in Paris. However, during the period from early June to early September, the liquid fraction remained essentially at 1 due to the high solar-air temperature. Consequently, there was few daily variation in the liquid fraction, as demonstrated in Fig. 7[e]. At this time the liquid PCM was unable to solidify and absorb heat, rendering it non-functional. So there was negligible difference in the indoor temperatures between the two types of houses. However, during spring and autumn these two transitional seasons, a higher daily difference in liquid fraction is shown in Fig. 7[e] compared to summer. Comparing this to Fig. 7[c], it becomes evident that the indoor temperature of the PCM concrete house was consistently lower than that of the normal concrete house during this period. For a

city with Guangzhou's climate characteristics, the proposed PCM concrete serves as an effective temperature regulator during the transitional seasons. Therefore, the spring period from early April to late May is chosen as the typical interval for further analysis.

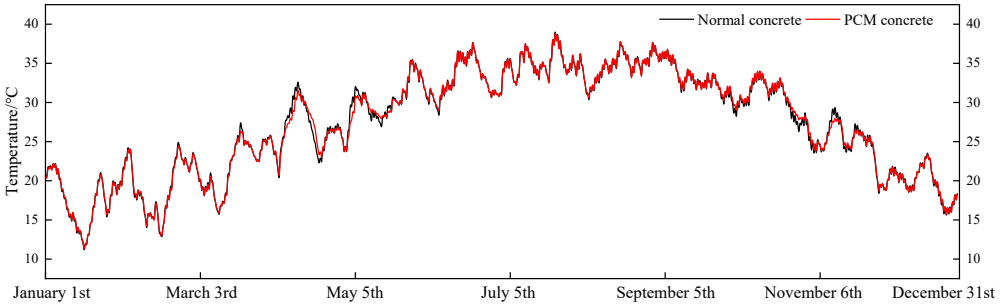

[c] Indoor temperature

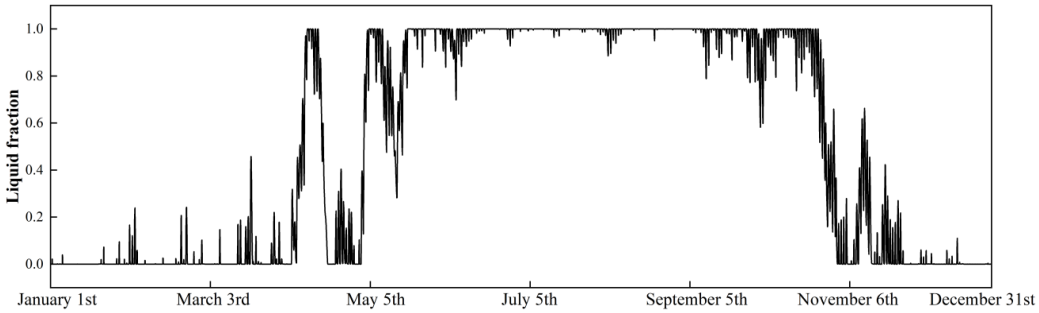

[d] Liquid fraction

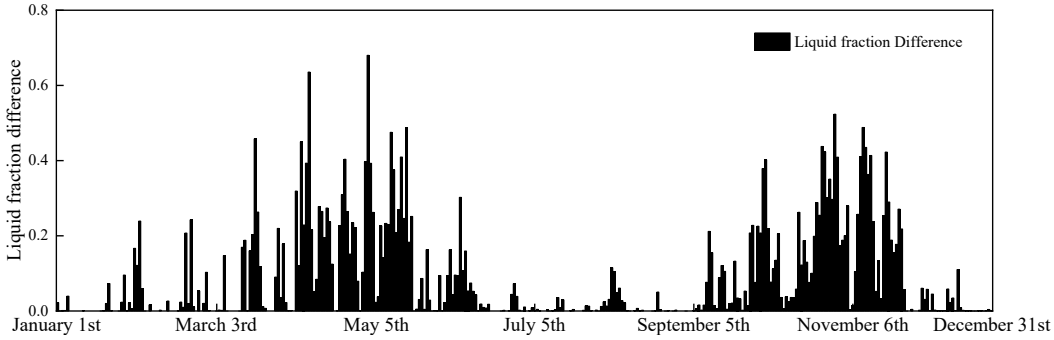

[e] Daily liquid fraction difference

Fig. 7 Full-year variations in [a] [b] [c] [d] [e] in Guangzhou

3.2.2 Typical interval analysis

Fig. 8[a] shows the average solar-air temperature, daily temperature difference between day and night, and liquid fraction variation in Guangzhou from April 5th to May 22nd (days). During this interval,about 22 days the solar-air temperature difference was greater than 20°C, accounting for 46.8% of the total duration. The average solar-air temperature difference during this interval was measured at 20.32°C. Meanwhile,the percentage of daily average solar-air

temperatures exceeding 25°C was found to be 86.96%. In contrast, the liquid fraction variation in Fig. 8[a] reveals significant and continuous fluctuations throughout this period, indicating a continuous phase change process within the PCM concrete. Combining this with the daily liquid fraction difference variation displayed in Fig. 8[b], it is observed that the difference exceeded 20% for 30 days, corresponding to approximately 65.22% of the interval. Thus, the PCM concrete is better utilized during this typical interval.

Fig. 8[c] and Fig. 8[d] compare the interior wall surface temperatures and indoor air temperatures for the normal concrete and PCM concrete houses during this period. In Fig 8[c], the average interior wall surface temperatures were measured at 28.01°C and 27.88°C for the normal concrete and PCM concrete houses,, with a maximum temperature difference of up to 2.24°C between them. The variance of the interior wall surface temperature was 6.24 and 4.73 for the normal concrete and PCM concrete houses respectively, highlighting the significant reduction in temperature fluctuation resulting from the application of PCM concrete. Additionally, the interior wall surface temperature exceeded 30°C for 296 hours in this interval for the normal concrete house, compared to 260 hours for the PCM concrete house. Consequently, the PCM concrete effectively reduced the duration of high interior wall surface temperature.

While in Fig. 8[d], which presents the indoor air temperature variation and temperature difference between the two types of houses, it can be observed that the overall trend aligns with the temperature variation observed on the interior wall surface. For the majority of the time, the indoor temperature of the PCM concrete house remained lower than that of the normal concrete house, reaching 691h, approximately 61.25% of the interval. The mean indoor air temperatures were 28°C and 27.87°C for the normal concrete and PCM concrete houses, with variances of 6.21 and 4.71 respectively. The indoor temperatures and temperature fluctuations of the PCM concrete house reduced significantly compared to the normal concrete house.

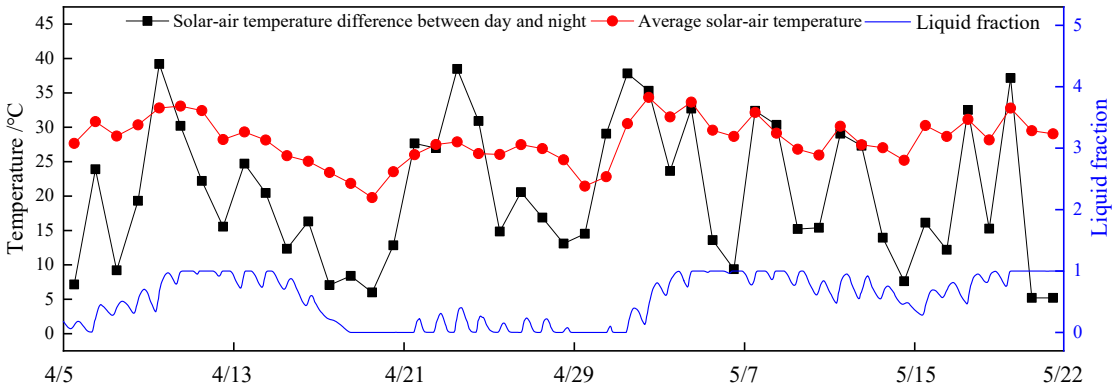

[a] Average solar-air temperature, daily temperature difference between day and night and liquid fraction

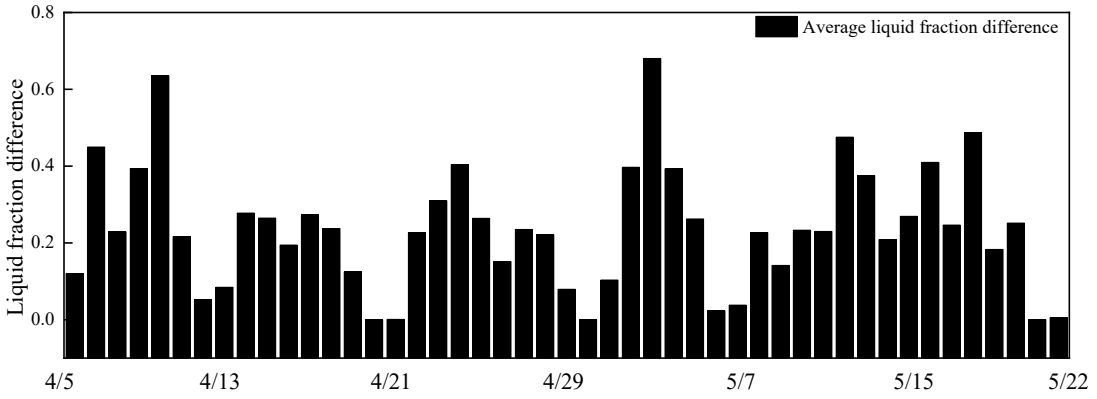

[b] Daily average liquid fraction difference

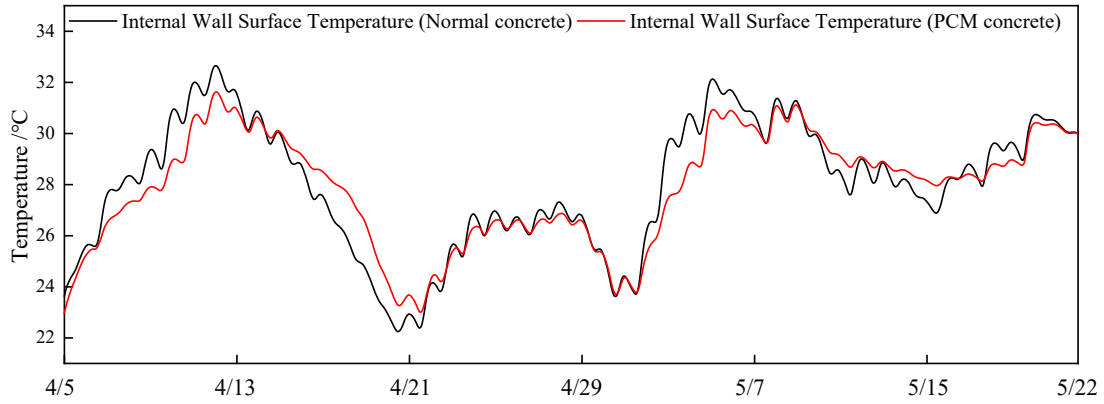

[c] Interior wall surface temperature variation

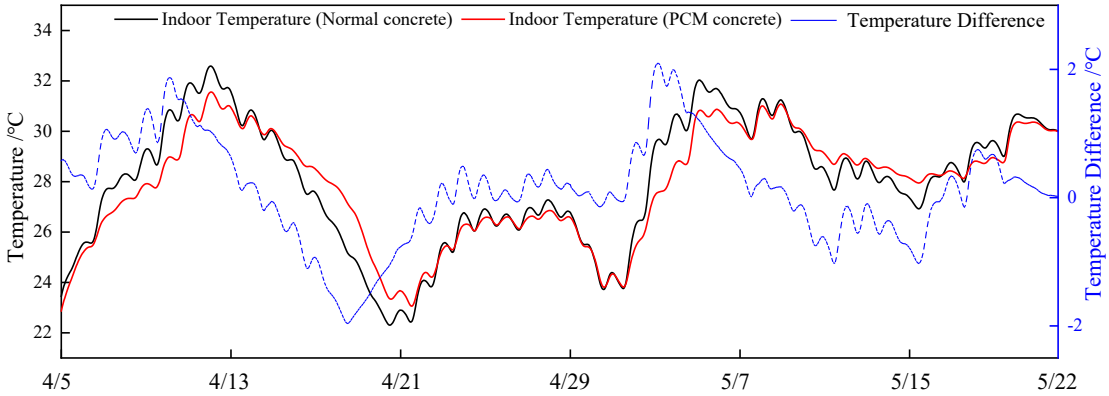

[d] Indoor temperature variation

Fig. 8 The variation of the [a] [b] [c] [d] between two houses in Guangzhou from April 5th to May 22nd

3.3 Beijing

3.3.1 Variation in indoor temperature and liquid fraction throughout the year

Beijing has a typical north temperate semi-humid continental monsoon climate with hot and rainy summers and cold and dry winters. The annual average temperature is 13°C and the average temperatures in January and July are about -4°C and 27°C. Fig. 9[a] shows the annual outdoor ambient temperature and solar horizontal radiation variation in the region, while Fig. 9[b] shows the daily average solar-air temperature.

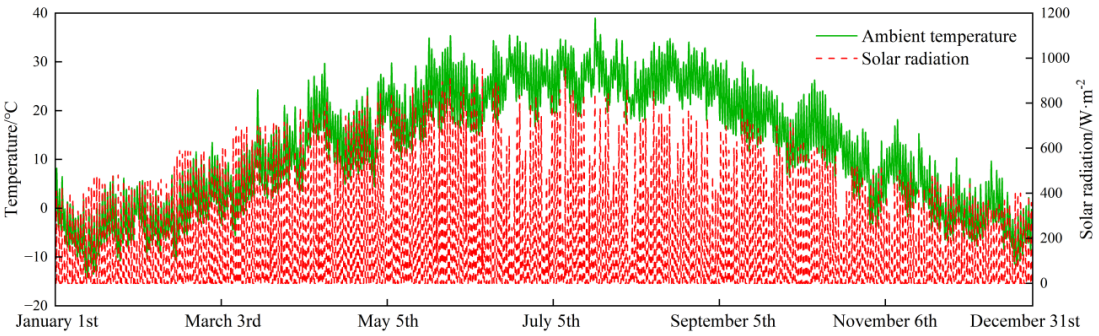

[a] Outdoor temperature and solar horizontal radiation

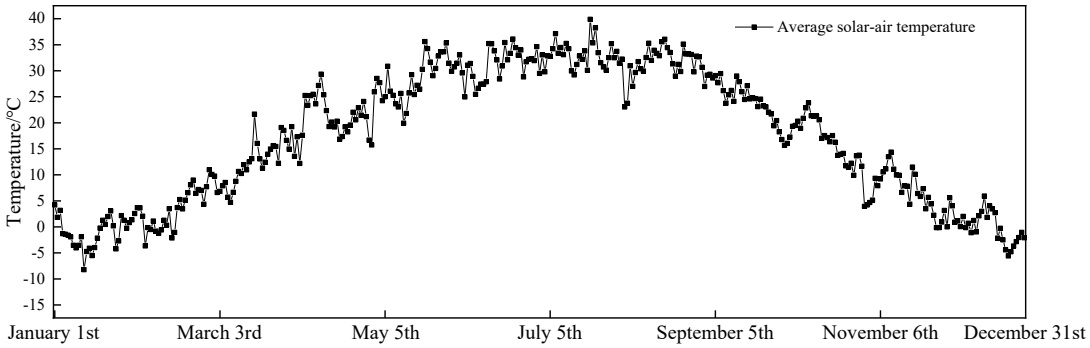

[b] Daily average solar-air temperature

Fig. 9[c] and Fig. 9[d] show the annual variation in indoor temperatures for both the normal concrete and PCM concrete houses, as well as the liquid fraction of PCM concrete in Beijing. Based on Fig. 9[c] and Fig. 9[d], it can be concluded that although the liquid fraction of the PCM concrete is higher in summer, exceeding 40% for 2737 hours (31% of the year) and surpassing 80% for 2270 hours (26% of the year), the

indoor temperature of the PCM concrete house does not significantly differ from that of the normal concrete house in summer. And in certain intervals, the indoor temperature of the PCM concrete house is even higher.This observation can be attributed to the excessively high average solar-air temperature in Beijing during the summer months (July to September), peaking at 909 hours above 30°C, representing 41.58% of the summer period. Consequently, the liquid fraction remains at an high value, rendering the PCM concrete in a molten state, thereby impeding solidification and heat absorption. Notably, in Beijing, only the period from mid-May to mid-June and mid-September throughout the year exhibit a more pronounced temperature regulation effect on PCM concrete. Therefore, this interval was selected as the typical interval for analysis.

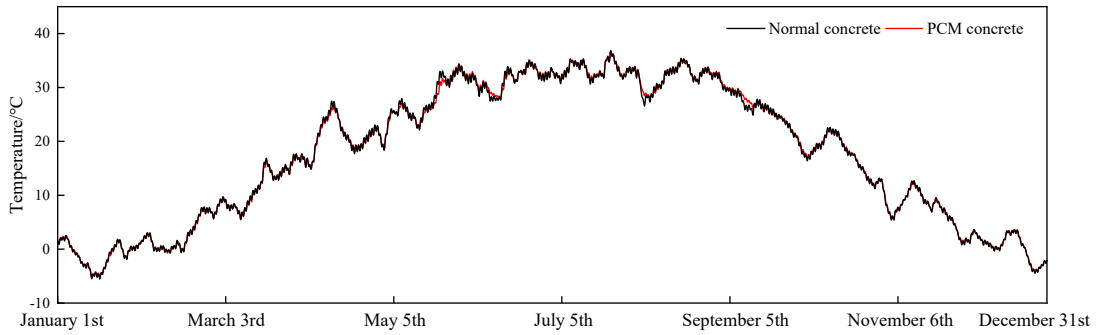

[c] Indoor temperature

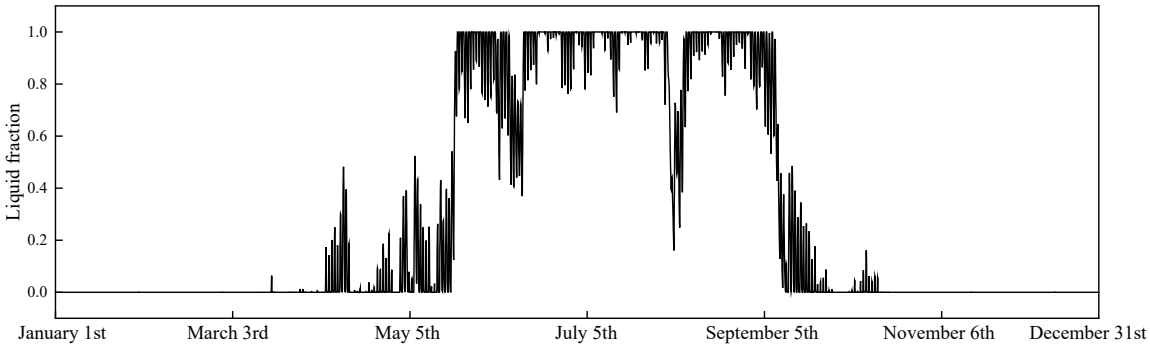

[d] Liquid fraction

Fig. 9. Full-year variations in [a] [b] [c] [d] in Beijing

3.3.2 Typical interval analysis

Fig. 10[a] displays the average solar-air temperature, daily temperature difference between day and night and liquid fraction variation in Beijing from May 5th to May 25th

(days). Despite the short duration, it is evident that the solar-air temperature between day and night in Beijing fluctuated greatly. During this interval, the temperature difference exceeded 20°C for approximately 90.48% of the time, spanning 19 days. Moreover, the temperature difference exceeded 30°C for approximately 71.43% of the time, encompassing 15 days, with an average temperature difference of 31.23°C. .Fig. 10[a] also demonstrates considerable variations in the liquid fraction, indicating the constant phase changes of PCM concrete as it regulates building temperatures.

Fig. 10[c] and Fig. 10[d] depict the comparison of the interior wall surface temperatures and indoor air temperatures for the normal concrete and PCM concrete houses during this period. According to Fig. 10[c], the average interior wall surface temperatures were 26.85 and 26.35 for the normal concrete and PCM concrete houses respectively, with variances of 7.85 and 5.59. The application of PCM concrete significantly reduced the interior wall surface temperature and temperature fluctuations. Notably, during this interval, the interior wall surface temperature of the normal concrete house exceeded 28°C for 121 hours, while the PCM concrete house experienced only 102 hours, effectively reducing the duration of high temperatures on the interior wall surface.

Fig. 10[d] illustrates the change in indoor air temperature between the two houses, with the PCM concrete house exhibiting lower indoor temperatures than the normal concrete house for 79.17% of the interval, amounting to 399 h. The maximum difference in indoor temperature between the PCM concrete house and the normal concrete house was 2.39°C. The average indoor air temperature of the normal concrete and the PCM concrete were 26.86°C and 26.35°C, with a variance of 7.97 and 5.66 respectively. These findings highlight the effective reduction in indoor temperature and temperature fluctuations achieved by utilizing PCM concrete.

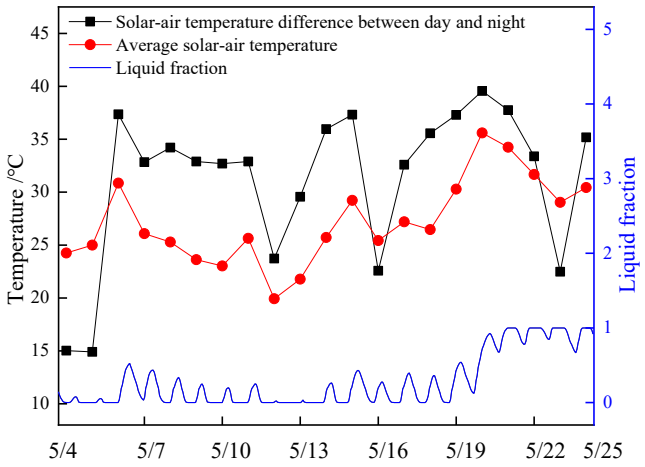

[a] Average solar-air temperature, daily temperature difference between day and night and liquid fraction

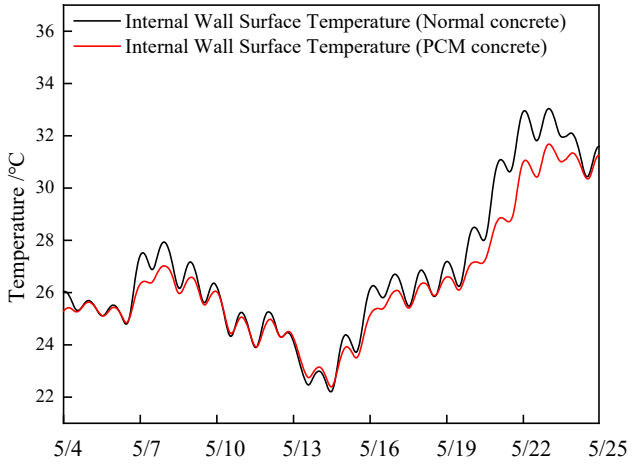

[b] Interior wall surface temperature

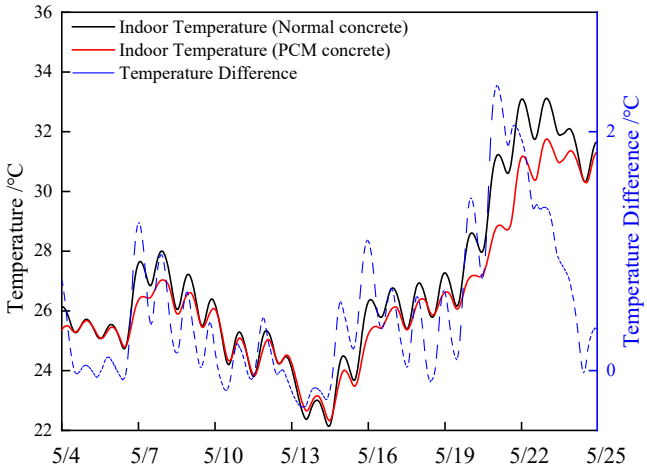

[c] Indoor temperature

Fig. 10. The variation of the [a] [b] [c] between two houses in Beijing from May 5th to May 25th

3.4 Hangzhou

3.4.1 Variation in indoor temperature and liquid fraction throughout the year

Hangzhou is the capital of Zhejiang Province, a hot-summer and cold-winter zone with a subtropical monsoon climate. The annual average temperature is 17.7°C and the average temperatures in January and July are about 5°C and 30°C. Fig. 11[a] illustrates the annual outdoor ambient temperature and solar horizontal radiation variation in the region, while Fig. 11[b] shows the daily average solar-air temperature.

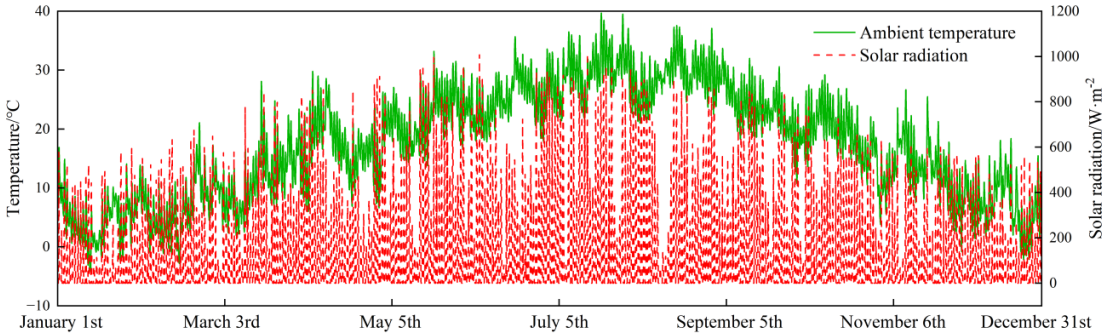

[a] Outdoor temperature and solar horizontal radiation

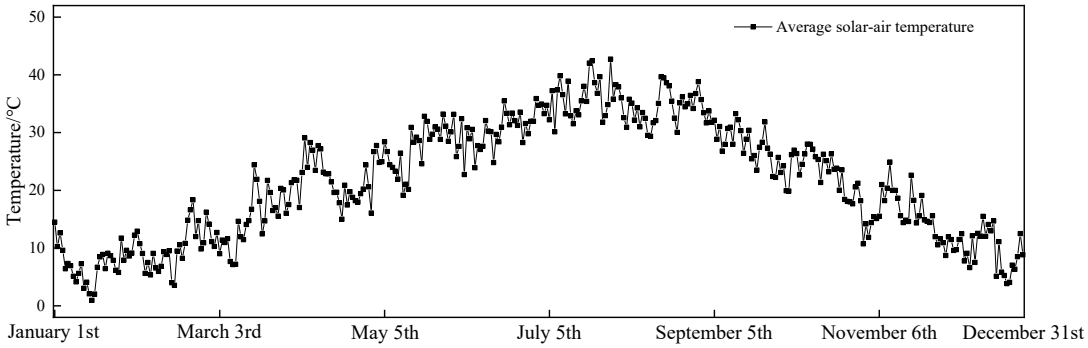

[b] Daily average solar-air temperature

Fig. 11[c] and Fig. 11[d] present the annual variation in indoor temperatures for both the normal concrete and PCM concrete houses, as well as the liquid fraction of PCM concrete in Hangzhou. Similar to Beijing, it can be observed from Fig. 11[c] and Fig. 11[d] that the average solar-air temperature during the summer months (July to September) was excessively high in Hangzhou as well, reaching 1418 hours above 30°C, accounting for approximately 64.93% of the summer period. This resulted in the PCM concrete remaining in a constant molten state with a high liquid fraction, but without significant fluctuations to effectively regulate indoor temperature.

Throughout most of the year, the indoor temperature of the two types of houses in Hangzhou was comparable. Although the indoor temperature of the normal concrete house exceeded than that of the PCM concrete house for 4050h, approximately 46.23% of the year, the temperature difference was mostly minimal. The time period with a more significant temperature difference was primarily concentrated from late April to late May and middle September to early and middle October. Hence, late April to late May was chosen as the typical interval for analysis.

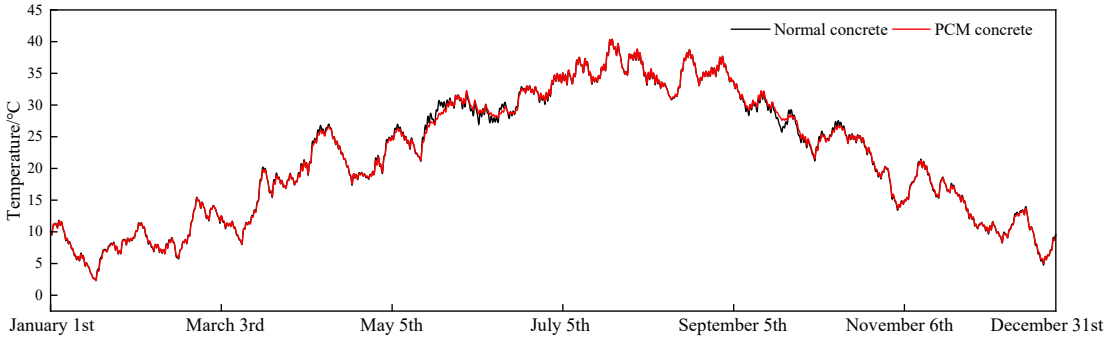

[c] Indoor temperature

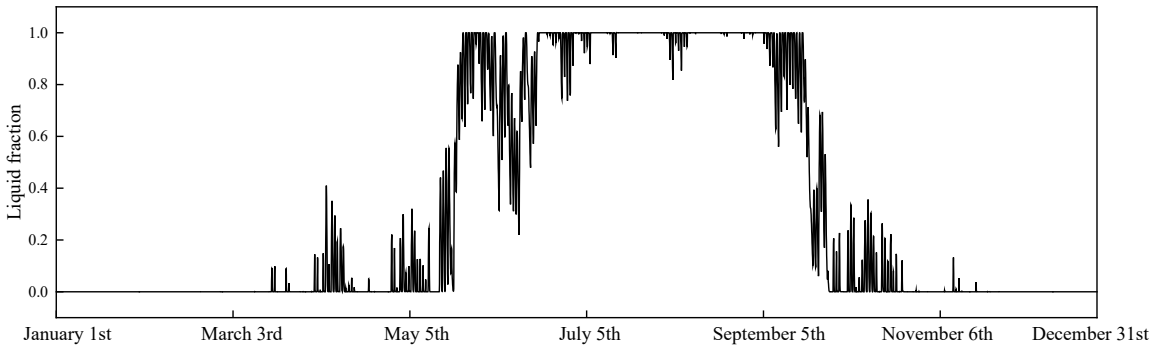

[d] Liquid fraction

Fig. 11 Full-year variations in [a] [b] [c] [d] in Hangzhou

3.4.2 Typical interval analysis

Fig. 12[a] illustrates the average solar-air temperature, daily temperature difference between day and night, and liquid fraction variation in Hangzhou area from April 29th to May 27th (days). During this time period, the solar-air temperature in the Hangzhou area fluctuated significantly between day and night, with periods greater exceeding 20°C lasting for 20 days and periods exceeding 30°C lasting for 13 days.

This duration accounted for 71.43% and 46.43% of the time period, respectively, representing a considerable portion. The average solar-air temperature difference during this interval was 26.74°C. Moreover, the proportion of time periods with a daily average solar-air temperature greater than 25°C was 57.14%. In Fig 12[a], the liquid fraction exhibits wide and continuous variations, indicating that the PCM concrete is constantly undergoing phase changes to regulate temperature.

Fig 12[c] and Fig 12[d] depict the comparison of the interior wall surface temperatures and indoor air temperatures for normal concrete and PCM concrete within this interval.Fig 12[c] shows that the interior side wall temperatures for the normal concrete and the PCM concrete were 25.67°C and 25.24°C,with variances of 9.76 and 7.81.The application of PCM concrete significantly reduced the interior side wall temperatures and temperature fluctuations. Additionally, the interior side wall surface temperature of the normal concrete exceeded 28°C for 29h during this interval, while the PCM concrete only reached 23h, thus shortening the duration of high temperatures for the interior side wall surface.

Fig. 12[d] shows the variation of indoor air temperature for the two houses. Within the interval, the indoor temperature of the PCM concrete house was lower than that of the normal concrete house for 77.83% of the time, amounting to 523 hours The maximum indoor temperature difference between the PCM concrete house and the normal concrete house was 2.08°C. The average indoor air temperature of the normal concrete house and the PCM concrete house were 25.66°C and 25.24°C,with variances of 9.69 and 7.78 respectively. These findings demonstrate that PCM concrete effectively reduces indoor temperature and temperature fluctuations.

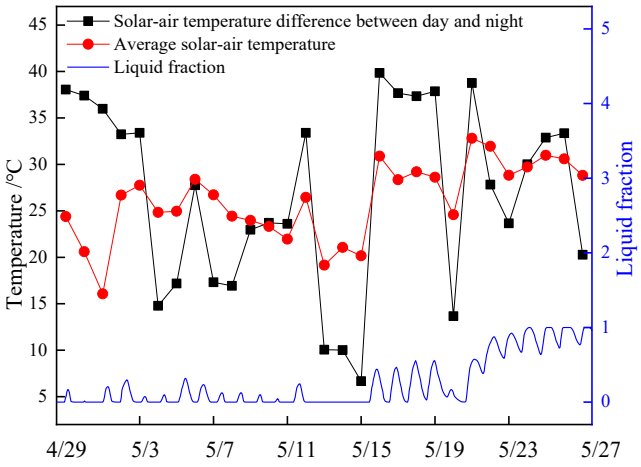

[a] Average solar-air temperature, daily temperature difference between day and night and liquid fraction

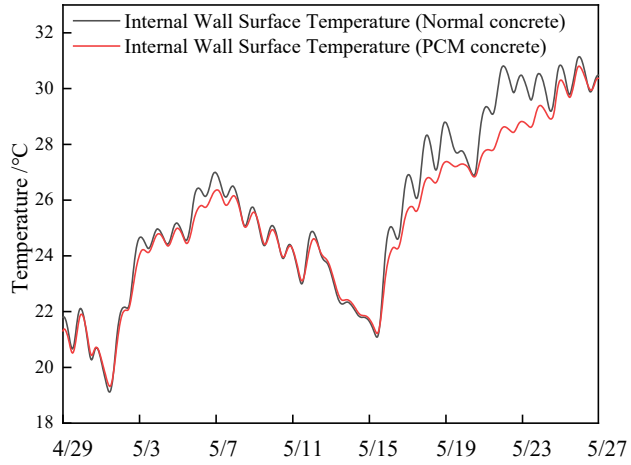

[b] Interior wall surface temperature

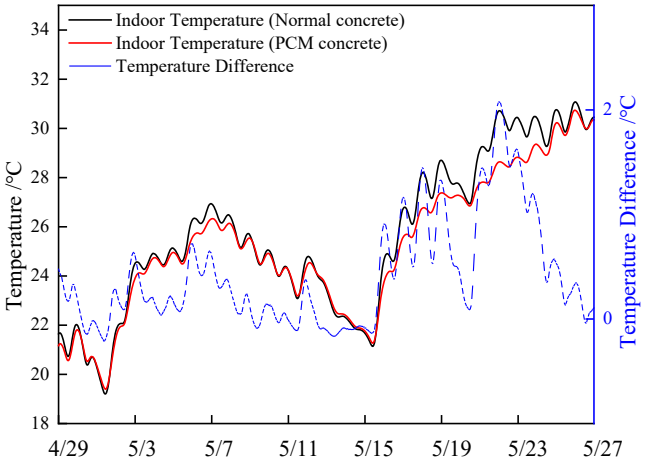

[c] Indoor temperature

Fig12 The variation of the [a] [b] [c] between two houses in Hangzhou from April 29th to May 27th

3.5 Summary

Summarizing the simulation results for four regions, it can be concluded that PCM

concrete performs optimally in Paris. Only in Paris can PCM demonstrate effectiveness during the summer months when the solar-air temperature reaches its peak. In the typical interval, the PCM concrete house maintains a lower indoor temperature than the normal concrete house for 1564 hours. Furthermore, the variance of the indoor air temperature is 4.01 for the normal concrete house and 3.20 for the PCM concrete house, indicating a significant reduction in temperature fluctuations with the use of PCM concrete.

In the remaining three cities, due to the high solar-air temperature in summer, the PCM in the wall remained in a molten state unable to solidify and absorb heat. The liquid fraction remained high, preventing the indoor temperature of the PCM concrete house from being lower than that of the normal concrete house. PCM concrete is only effective during transitional seasons like spring and autumn in these cities. In the typical interval in Guangzhou, the indoor temperature of the PCM concrete house is lower than that of the normal concrete house for 691 hours. In contrast, the typical intervals in Beijing and Hangzhou are only 399 h and 523h. The variance of the indoor air temperature of the normal concrete house and PCM concrete house in Guangzhou is 6.21 and 4.71 respectively, while in Beijing is 7.97 and 5.66,and in Hangzhou is 9.69 and 7.69, respectively.

Additionally, a comparison of the liquid fraction and the average room temperature for each month of the year reveals that the effectiveness of PCM is not consistent throughout the year, as the solid phase temperature influences the melting process of PCM. When the maximum and minimum temperatures surpass the solid phase temperature, PCM completely melts, and vice versa. The average indoor temperature decreases as the liquid fraction of PCM increases. Higher liquid fractions lead to greater temperature differences between normal concrete houses and PCM concrete houses,

indicating that PCM melts to absorb and store heat, resulting in reduced temperature rise for most of the time. Even in months when PCM is not actively functioning, there remains a temperature difference between normal concrete houses and PCM concrete houses due to the higher heat capacity and lower thermal conductivity of PCM concrete.

Comparative analysis of the effects of PCM concrete application in these four different regions demonstrates that the thermal performance of PCM concrete is primarily influenced by the daily solar-air temperature and the temperature difference between day and night. These factors determine whether PCM concrete can undergo a phase change process, providing latent heat, and whether it can solidify through a reduction in solar-air temperature to progress to the next cycle of the phase change process. This novel PCM concrete performs optimally at solar-air temperatures of 26-28°C.

These results highlight the importance of selecting PCM concrete with suitable phase change temperature zones for different climate regions. Appropriate phase change temperature zones enhance the effective utilization of PCM concrete, maximize latent heat storage, and allow the phase change zone to adjust with solar-air temperature fluctuations, ensuring the completion of the cyclic phase change process (melting-solidifying-melting). The incorporation of PCM concrete reduces heat transfer through the wall, showing significant thermal management capabilities.

Table 3 Application effect of PCM concrete in four cities

City	Significant application effect interval (Day/Month)	Duration of reducing indoor air temperature (hour)	Indoor air temperature variance of normal concrete	Indoor air temperature variance of PCM concrete
Paris	12/6-7/10	1564	4.01	3.20
Guangzhou	5/4-22/22	691	6.21	4.71
Beijing	5/5-25/5	399	7.97	5.66

Hangzhou	29/4-27/5	523	9.69	7.69

4. Conclusion

This study aimed to simulate and analyze the thermal performance of a novel PCM concrete applied for buildings in four different climatic zones. The main conclusions are as follows:

(1) The heat transfer model considering the phase change process, was successfully established and validated by comparing it with experimental data. The high validity and accuracy of the model were confirmed through this rigorous validation process. Based on this study, a comprehensive heat transfer model was developed for a 3D house with a multi-storey envelope utilizing PCM concrete. The simulation studies were subsequently conducted using the thermal conductivity control equation described above.

(2) In Paris, where the liquid fraction exhibited variations and fluctuations during summer, the PCM concrete house consistently maintained a significantly lower indoor temperature than the normal concrete house for 1564 hours. The reduced variance of 0.81 contributed to a decrease in temperature fluctuations. Conversely, in winter, the distinct physical properties of PCM concrete resulted in a higher indoor temperature compared to normal concrete. The PCM concrete house achieved a thermal regulation effect, with higher temperatures in winter and lower temperatures in summer, thereby providing favorable thermal comfort for occupants.

(3) In Guangzhou, Beijing, and Hangzhou, the high solar-air temperature during summer prevented PCM from solidifying and absorbing heat, leaving the PCM in a molten state with a high liquid fraction. As a result, PCM concrete was effective only during the spring and autumn, unable to reduce indoor temperatures in summer.

(4)A comparison of the application effects of the novel PCM concrete in four regions shows that the addition of novel PCM concrete can reduce the heat transfer through the wall. However, the comprehensive daily solar-air temperature is the primary factor influencing the temperature regulation effect of PCM concrete. To optimize performance in different climate zones, suitable PCM materials with phase change temperature zones must be selected. A well-chosen phase change temperature zone enhances the effective utilization of PCM concrete, maximizes latent heat storage, and enables smooth completion of the melting-setting-melting phase change process by adjusting to solar-air temperature fluctuations. The novel PCM concrete can be effective at a combined outdoor temperature of 26-28°C. In the future work, a suitable thermal comfort indicator should be proposed to evaluate the effectiveness of PCM applications in buildings, and more PCM building materials should be studied for different climate zones to investigate the optimal approach of PCM application in varied climate conditions.

5. Acknowledgements

This work was supported by the National Natural Science Foundation of China (NSFC) (No. 52006146).

6. References

[1] Kondo T, Tadahiko T, Yuuji T. Research on the Thermal Storage of PCM Wallboard[J]. IEA Annex 10.5th Workshop, 2001,(01):1-9.

[2] Koschenz M, Lehmann. B. Development of a themally activated ceiling panel with PCM for application in lightweight and retrofitted buildings[J]. Energy and Buildings, 2004, 36(6):567-578.

[3] Sait H H. Experimental study of water solidification phenomenon for ice-on-coil thermal energy

storage application utilizing falling film[J]. Applied Thermal Engineering, 2019,146:135-145.

[4] M.A. Izquierdo-Barrientos,J.F. Belmonte,D. Rodríguez-Sánchez,A.E. Molina,J.A. Almendros-Ibáñez. A numerical study of external building walls containing phase change materials (PCM)[J]. Applied Thermal Engineering,2012,47.

[5] Silva T, Vicente R, Soares N, et al. Experimental testing and numerical modelling of masonry wall solution with PCM incorporation: A passive construction solution[J]. Energy and Buildings, 2012, 49: 235-245.

[6] Silva T, Vicente R, Rodrigues F, et al. Development of a window shutter with phase change materials: Full scale outdoor experimental approach[J]. Energy and Buildings, 2015, 88: 110-121.

[7] Royon L, Karim L, Bontemps A. Thermal energy storage and release of a new component with PCM for integration in floors for thermal management of buildings[J]. Energy & Buildings, 2013,63:29-35.

[8] Kośny J, Biswas K, Miller W, et al. Field thermal performance of naturally ventilated solar roof with PCM heat sink[J]. Solar Energy, 2012,86(9):2504-2514.

[9] Cui H, Tang W, Qin Q, et al. Development of structural-functional integrated energy storage concrete with innovative macro-encapsulated PCM by hollow steel ball[J]. Applied Energy, 2017, 185: 107-118.

[10] Bake Maitiniyazi,Shukla Ashish,Liu Shuli. Development of gypsum plasterboard embodied with microencapsulated phase change material for energy efficient buildings[J]. Materials Science for Energy Technologies,2021(prepublish).

[11] Becker R. Improving thermal and energy performance of buildings in summer with internal

phase change materials[J]. Journal of Building Physics, 2014,37(3):296-324.

[12] Sun Jingmeng,Zhao Junqi,Zhang Weiye,Xu Jianuo,Wang Beibei,Wang Xuanye,Zhou Jun,Guo Hongwu,Liu Yi. Composites with a Novel Core–shell Structural Expanded Perlite/Polyethylene glycol Composite PCM as Novel Green Energy Storage Composites for Building Energy Conservation[J]. Applied Energy,2023,330(PA).

[13] Saffari Mohammad,Roe Conor,Finn Donal P.. Improving the building energy flexibility using PCM-enhanced envelopes[J]. Applied Thermal Engineering,2022,217.

[14] Liu Lisa,Hammami Nadia,Trovalet Lionel,Bigot Dimitri,Habas Jean-Pierre,Malet-Damour Bruno. Description of phase change materials (PCMs) used in buildings under various climates: A review[J]. Journal of Energy Storage,2022,56(PA).

[15] Liu Zu-An,Hou Jiawen,Chen Yu,Liu Zaiqiang,Zhang Tao,Zeng Qian,Dewancker Bart Julien,Meng Xi,Jiang Guanzhao. Effectiveness assessment of different kinds/configurations of phase-change materials (PCM) for improving the thermal performance of lightweight building walls in summer and winter[J]. Renewable Energy,2023,202

[16] Al-Yasiri Qudama,Szabó Márta. Experimental study of PCM-enhanced building envelope towards energy-saving and decarbonisation in a severe hot climate[J]. Energy & Buildings,2023,279.

[17] Georgiou Loucas,Konatzii Panagiota,Morsink-Georgali Phoebe-Zoe,Klumbyte Egle,Christou Petros,Fokaides Paris A.. Numerical and environmental analysis of post constructive application of PCM coatings for the improvement of the energy performance of building structures[J]. Construction and Building Materials,2023,364.

[18] Liu Zu'an,Hou Jiawen,Wei Dong,Meng Xi,Dewancker Bart Julien. Thermal performance

analysis of lightweight building walls in different directions integrated with phase change materials (PCM)[J]. Case Studies in Thermal Engineering,2022,40.

[19] Kitagawa Haruka,Asawa Takashi,Kubota Tetsu,Trihamdani Andhang Rakhmat. Numerical simulation of radiant floor cooling systems using PCM for naturally ventilated buildings in a hot and humid climate[J]. Building and Environment,2022,226.

[20] Li Qing,Ju Zhipeng,Wang Zhiguo,Ma Lingyong,Jiang Wei,Li Dong,Jia Jiaojio. Thermal performance and economy of PCM foamed cement walls for buildings in different climate zones[J]. Energy & Buildings,2022,277.

[21] LI, Z. X., AL-RASHED, ABDULLAH A. A. A., ROSTAMZADEH, MAHFOUZ, et al. Heat transfer reduction in buildings by embedding phase change material in multi-layer walls: Effects of repositioning, thermophysical properties and thickness of PCM[J]. Energy conversion & management,2019,195(Sep.):43-56. DOI:10.1016/j.enconman.2019.04.075.

[22] J. Xie, W. Wang, J. Liu, S. Pan, Thermal performance analysis of PCM wallboards for building application based on numerical simulation, Solar Energy. 2018, 162: 533–540.

[23] Peng L,Wei W,Bin D, et al. Study on the heat and moisture transfer characteristics of aerogel-enhanced foam concrete precast wall panels and the influence of building energy consumption[J]. Energy & Buildings,2022,256.

[24] Hongtao He,Pin Zhao,Qinyan Yue,Baoyu Gao,Dongting Yue,Qian Li. A novel polynary fatty acid/sludge ceramsite composite phase change materials and its applications in building energy conservation[J]. Renewable Energy,2015,76.

[25] Zhang Yangkai,Sang Guochen,Du Xiaoyun,Cui Xiaoling,Zhang Lei,Zhu Yiyun,Guo Teng. Development of a novel alkali-activated slag-based composite containing paraffin/ceramsite shape stabilized phase change material for thermal energy storage[J]. Construction and

Building Materials,2021,304.

[26] Yingying Yang,Weidong Wu,Shunyu Fu,Hua Zhang. Study of a novel ceramsite-based shape-stabilized composite phase change material (PCM) for energy conservation in buildings[J]. Construction and Building Materials,2020,246(C)